LAWRENCE
LIVERMORE
NATIONAL
LABORATORY

UCRL-CONF-208109

Performance of Thin Borosilicate Glass Sheets at 351-nm

P. K. Whitman, D. Hahn, T. Soules, M. Norton, S. Dixit, G. Donohue, J. Folta, W. Hollingsworth, M. Mainschein-Cline

November 18, 2004

Boulder Damage Symposium XXXVI Annual Symposium on Optical Materials for High Power Lasers
Boulder, CO, United States
September 20, 2004 through September 22, 2004

Performance of Thin Borosilicate Glass Sheets at 351-nm

P.K.Whitman*, D. Hahn, T. Soules, M. Norton, S. Dixit, G. Donohue, J. Folta, W. Hollingsworth, M. Mainschein-Cline

University of California, Lawrence Livermore National Laboratory,
7000 East Avenue L-491, Livermore, California 94550, U.S.A.
UCRL-CONF-208109

ABSTRACT

Previously, we reported preliminary results for commercial thin borosilicate glass sheets evaluated for use as a frequently-replaced optic to separate the radiation and contamination produced by the inertial confinement fusion experiments in the National Ignition Facility target chamber from the expensive precision laser optics which focus and shape the 351-nm laser beam. The goal is identification of low cost substrates that can deliver acceptable beam energy and focal spots to the target. The two parameters that dominate the transmitted beam quality are the transmitted wave front error and 351-nm absorption. Commercial materials and fabrication processes have now been identified which meet the beam energy and focus requirements for all of the missions planned for the National Ignition Facility. We present the first data for use of such an optic on the National Ignition Facility laser.

Keywords**:** borosilicate glass, non-linear absorption, ultra-violet light, inclusions

1. INTRODUCTION

Commercial thin borosilicate glass sheets have been evaluated for use as a single-shot optic "debris shield" to separate the radiation and contamination produced by the inertial confinement fusion (ICF) experiment from the expensive precision laser optics which focus and shape the 351-nm laser beam which irradiates the target. The most promising commercial glasses that are potentially suitable for a disposable optical debris shield on the National Ignition Facility (NIF) laser are high purity borosilicate glasses. These glasses have good optical transmission, good resistance to thermal shock and are commercially available at high volume in sheet thicknesses and cost of interest for NIF. However, they often contain large bulk flaws –bubbles and knots (high silica inclusions with a different index than the surrounding glass) -- which could potentially reduce the useful lifetime. In addition, earlier screening experiments[1] suggested that fluence-dependent transmittance losses could occur when borosilicate glass sheets are irradiated with 351-nm laser pulses at high intensity (2 – 4 GW/cm^2). This study was undertaken to more carefully quantify both temporal and permanent losses in Schott Borofloat®33 borosilicate glass sheets, which are the leading candidate for use on the NIF laser.

2. EXPERIMENT

2.1 Materials

Samples of Borofloat®[1]33, a commercial sodium-aluminum-borosilicate glass were obtained from Schott Glass (Jena, Germany). The sub-aperture test sample surfaces were cleaned using standard NIF protocols, but otherwise tested as received – i.e. float glass surfaces. These samples were not anti-reflection coated before testing. The full-aperture optics installed on the National Ignition Facility (NIF) laser were mechanically polished after forming, cleaned and coated with ammonia-hardened porous silica sol-gel anti-reflection coating designed for use at 351-nm[2].

* Correspondence: Email: whitman2@llnl.gov; Telephone: 925 424 3583; Fax: 925 423 5xxx

[1] Schott North America Corporation, Elmsford, NY

2.2 Measurement of 355-nm transmittance

The Small Optics Test (SOT) facility was reconfigured to measure the temporal and permanent absorption losses. A Coherent Infinity Q-switched tripled Nd:YaG laser provided the test beam [355nm (3.9ns, FWHM)]. The laser produces a spot that is ~ 1.0 mm diameter at the $1/e^2$ point and has Gaussian temporal and spatial profile. The incident and transmitted beam energy was measured before and after the test sample using NIST-calibrated Molectron J-50 energy probes. Photodiodes placed before and after the sample provided temporal profiles. All fluences (energy per cm^2 per pulse) are quoted at the peak of the beam profile as measured with a Coherent beam view analyzer. With this configuration it was possible to measure the integrated sample transmission and any substrate-induced modification of the laser temporal pulse. Figure 1 shows the layout for this experiment.

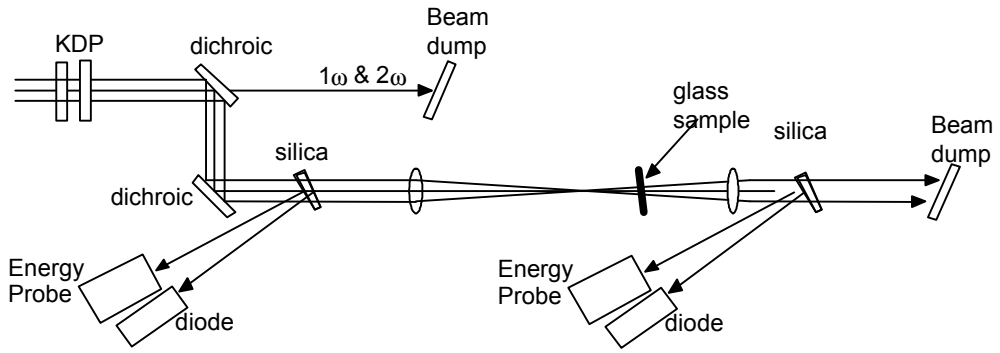

Figure 1. Experimental arrangement for measuring transmission loss using the Coherent Infinity laser at 355-nm.

2.2. 1. Optical measurements set-up for 355 nm

In order to determine the linear and non-linear absorption of the Borofloat®33 samples we measured the transmittance as a function of fluence. The main laser shot fluence was incremented from 2 to 14 J/cm^2 in 2 J/cm^2 increments. Twenty measurements, each at a virgin location, were made for each test fluence. The main laser shot, as it is ramped from 2 to 14 J/cm2, will develop the non-linear coefficient. To determine if the laser had induced any damage to the plate, we added 10 low energy (2 J/cm^2) shots before and after each main shot. Comparing the pre and post shots indicates whether there was a permanent change in the substrate. The series was stopped if the post-shot transmissions indicated that the laser was producing damage.

In order to determine the linear absorption coefficient at low power, measurements were also made with a Cary 500i spectrophotometer operating in dual-beam mode. The instrument was fitted with a mirror arrangement in the sample beam that enabled examination of any point on the surface of the samples. Single-wavelength transmittance measurements were made at 350 nm and at 355 nm on the 15-cm-square samples. Immediately prior to taking each single-wavelength measurement, the spectrophotometer was calibrated using air as a 100% transmittance standard. Each single-wavelength result was the average of five measurements, each taken over a 10-second integration time. In addition to the single-wavelength measurements, the transmittance spectra of all four samples were obtained over the range 800 nm to 250 nm. Immediately prior to obtaining each spectrum, a spectrophotometric baseline was obtained, again using air as the 100% transmittance standard.

Later these three samples were put through a buffered HF etching process to remove ~1μm from the surface and re-cleaned. The experiment was then repeated using the same procedure in a previously unexposed area.

.

2.2. 2. Composition measurements

Because iron absorption in the UV is expected to be the source of the linear and non-linear absorption at 355 nm, the composition of each of the three different thickness Borofloat®33 samples was determined by XRF. The measurements were made on an Omicron by Thermo-Noran (Kevex). NBS borosilicate glass samples SRM 93A and 1411 were used as reference. Particular attention was paid to the concentration of iron. Table 1 gives the elemental and oxide concentrations determined by XRF on the three samples of different thickness: 0.118 (A), 1.09 (B) and 2.08 cm (C).

Boron concentrations could not be determined by XRF and so were fixed at levels obtained in previous measurements by ICP/MS on an earlier sample. Small changes in the boron level would not affect ratios of the other oxides.

Table 1. Composition of the samples for transmission measurement experiments.

El	line	Intensity (counts)			Conc. (wt %)			Oxide	Conc. (wt %)			Error (1 sigma)		
		A	B	C	A	B	C		A	B	C	A	B	C
B	Kα	--	--	--	3.99	3.99	3.99	B_2O_3	12.9	12.9	12.9	--	--	--
Na	Kα	23.5	23.2	23.3	2.68	2.64	2.65	Na_2O	3.61	3.56	3.58	0.06	0.06	0.06
Al	Kα	132	132	130	1.42	1.41	1.39	Al_2O_3	2.67	2.66	2.63	0.02	0.02	0.02
Si	Kα	5882	5879	5906	38.9	38.9	39.0	SiO_2	83.2	83.1	83.5	0.06	0.06	0.06
K	Kα	117	122	131	0.47	0.48	0.52	K_2O	0.56	0.58	0.62	0.00	0.00	0.00
Fe	Kα	1.35	1.16	2.31	3.51 ppm	3.02 ppm	6.11 ppm	Fe_2O_3	5.01 ppm	4.32 ppm	8.73 ppm	0.33	0.40	0.46
Zr	Kα	59.5	63.4	69.3	287 ppm	306 ppm	342 ppm	ZrO_2	0.04	0.04	0.05	0.00	0.00	0.00

2.3 Measurement of the impact of bulk flaws on laser performance

The test pieces were shot at 3ω in 10 torr of dry air in the SLAB lab facility. The laser is the SLAB laser system[3]: a Nd: glass zigzag slab amplifier, with SBS phase conjugation producing a near diffraction limited 1.053 μm output. As used for these experiments it provides a 6 J, 351 nm, 6 mm x 6 mm square beam, with a 10 ns FWHM near Gaussian pulse, at a rep rate of 0.5-Hz. This rep rate is limited by data collection rate, as the laser system can be operated at 5 Hz. The test setup is shown schematically in figure 2. The 1-μm output of the SLAB laser is image-relayed to the frequency converter on the experiment table. The 3ω output of the frequency converter is spatially filtered and image-relayed to the sample plane in the vacuum test chamber. The incidence angle is 15º. The sample fluence was set with the input 3ω NF 16-bit scientific-grade camera, which was calibrated for energy and magnification to yield the fluence on target. The transmitted beam is captured on each shot while monitoring the site for growth or initiation of damage anywhere else in the whole beam. A long working distance microscope image, which views the exit surface at 15º, is also captured on

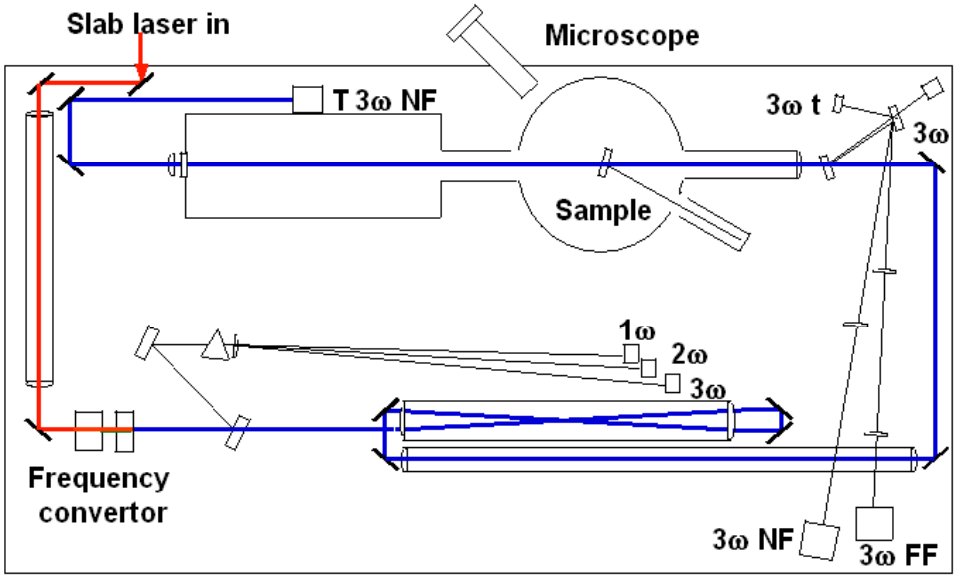

Figure 2. Layout for testing inclusions on the SLAB laser.

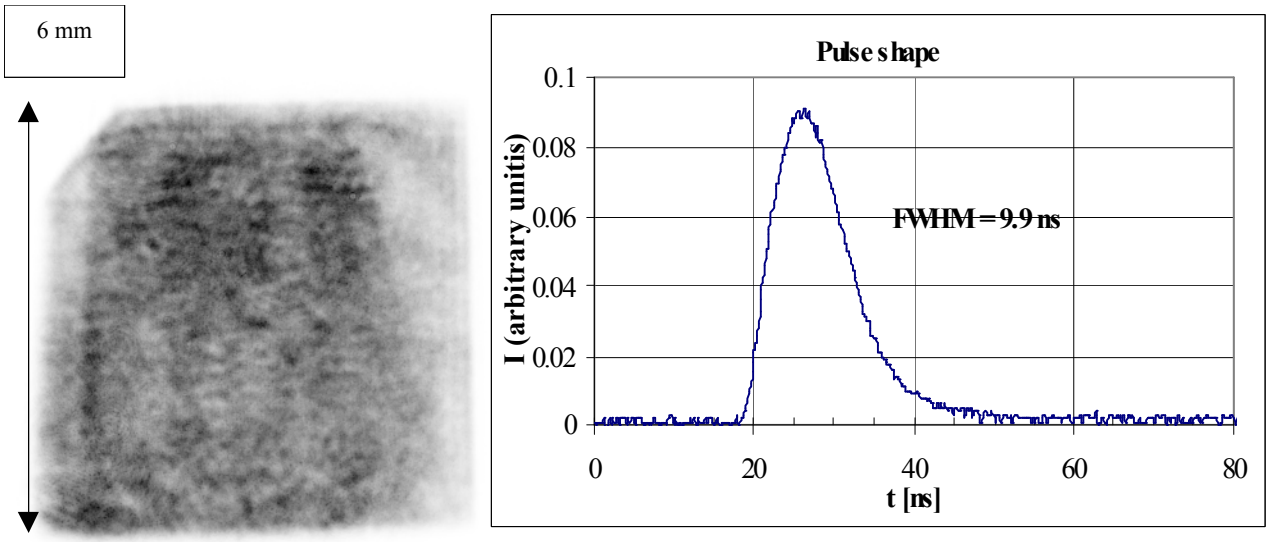

Figure 3. Typical beam near field and typical temporal pulse trace.

each shot. The beam area on the test piece is 0.3 cm^2 and the average temporal pulse is 10 ns FWHM. A typical near field and typical temporal pulse shape are shown in figure 3. The measured FWHM has been corrected for a systematic error introduced in the measurement electronics.. The f/# of the test chamber optical system is 100. The contrast ratio of the patch surrounding the test site is 10%, whereas the contrast ratio in the central 65% of the beam area is 25%.

Prior to laser exposure, photomicrographs were taken of each defect using a high-resolution microscope; size, location, type of defect, and magnification were recorded. Four bubbles, and four knots were photographed (only five sites were tested). As the laser fluence was slowly ramped from ~ 1 to 10 J/cm^2 at the defect site, beam statistics, low-resolution microscope images of the defect, and notes as to the behavior of the glass at the defect site were recorded. After laser exposure, high-resolution micrographs of each defect were again taken to compare to the original.

3. RESULTS AND ANALYSIS

3.1 Transmittance of a 355-nm Gaussian pulse

3.1 1. Background Theory

Attenuation of an optical pulse *I(r,z,t)* as it propagates through a non-linear material is described by the relation

$$\frac{dI}{dz} = -(\alpha[Fe] + \beta[Fe]I + s)I. \qquad (1)$$

where α is the linear absorption coefficient, β is the non-linear or two-photon absorption coefficient, [Fe] is the concentration of ferrous and ferric ions in ppm. A good fit to the linear and non-linear absorption was obtained when the absorption coefficients are taken to be proportional to the iron concentration. s accounts for irreversible damage to the optic and depends on the history. When post shots showed a drop in transmission the optic is damaged and the data is not recorded at this fluence.

Integrating Eq. 1 between two surfaces of a flat plate and including only single reflections at each surface gives

$$\frac{I}{I_0} = T_{lin}\left[\frac{1}{1+Q}\right]. \qquad (2)$$

where

$$T_{lin} = (1-R)^2 \exp(-\alpha[Fe]L);$$

is the ordinary linear absorption for a plate of thickness L and single surface reflection R. The second term accounts for the non-linear or two-photon absorption,

$$Q = I\left(\frac{\beta}{\alpha}\right)\left[1-\exp(-\alpha[Fe]L)\right].$$

For a pulse that is constant in intensity perpendicular to the beam direction and rectangular in time, Eq. 2 describes the transmission. However, in the general case, the intensity I is a function not only of thickness but also of time, t, and the direction perpendicular to the beam direction or the transverse position, r. Hence for a general circular beam shape the total beam pulse transmission is given by

$$T = \frac{\int_{-\infty}^{\infty} dt \int_{0}^{\infty} 2\pi dr I(r,L,t)}{\int_{-\infty}^{\infty} dt \int_{0}^{\infty} 2\pi dr I(r,0,t)}. \qquad (3)$$

For the Coherent Infinity laser used here which has an initial pulse that is approximately Gaussian in time and has a circular intensity profile perpendicular to the beam that falls off as a Gaussian in r, so that I_0 is proportional to $\exp(-a\,t^2 - b\,r^2)$ substituting into Eq. 3 gives[4],

$$T = T_{lin}\frac{2}{\sqrt{\pi}\,Q}\int_{0}^{\infty}\ln\left(1+Qe^{-x^2}\right)dx. \qquad (4)$$

For a beam, such as, the NIF beam whose intensity is approximately constant in space perpendicular to the beam but whose pulse is Gaussian in time,

$$T = T_{lin}\frac{1}{\sqrt{\pi}}\int_{-\infty}^{\infty}\frac{e^{-x^2}}{1+Qe^{-x^2}}dx. \qquad (5)$$

3.1 2. Optical Performance of Borofloat® 33 Glass at 355 nm

Figures 4, 5, and 6 graph the total transmission of laser pulses through the Borofloat®33 plates of different thickness as a function of the laser pulse intensity. Data points shown are for the main pulse measured as discussed above. Each sample had a portion of the plate etched with hydrofluoric acid to remove a thin layer from the surface and any surface contaminants in that layer. Fig. 4 shows results of transmission through an etched portion of each plate. Fig. 5 shows data through a non-etched portion. Fig. 6 shows the combined data. The combined data shows that etching did not have a significant effect on transmission through the thinner samples. However, it did appear to improve transmission on the positions investigated in the thicker sample perhaps by removing some surface contaminant.

The values at near zero fluence were measured using the Cary 300i spectrophotometer as described above. These are shown in Figure 7. The sharp absorption peak at ~ 380nm, particularly evident in the spectra of the thickest samples, is characteristic of the presence of iron in silicate glasses. There is no significant difference in the spectra with or without etching.

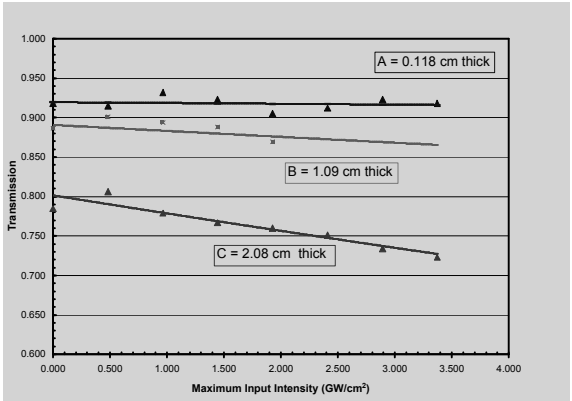

Figure 4. Transmission data obtained on the Borofloat®33 glass plates when the laser was positioned so as to pass through an etched portion of each plate. The best-fit values for α and β are 0.011 cm^{-1} [Fe ppm]$^{-1}$ and 0.008 cm GW^{-1} [Fe ppm]$^{-1}$ respectively.

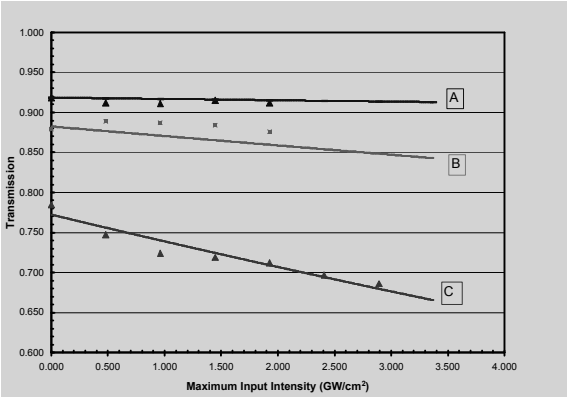

Figure 5. Transmission data when the laser was positioned so as to pass through a non- etched portion of each plate. The best-fit values for α and β are 0.014 cm^{-1} [Fe ppm]$^{-1}$ and 0.013 cm GW^{-1} [Fe ppm]$^{-1}$ respectively.

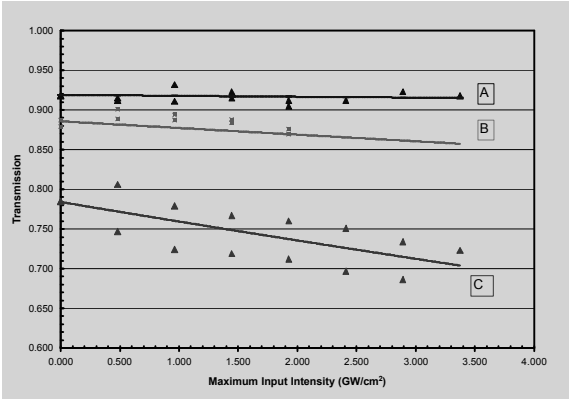

Figure 6. Combined experimental transmission data from Fig. 4 and Fig 5. The values of the linear and non-linear parameters were re-optimized. α = 0.01 cm^{-1} [Fe ppm]$^{-1}$ and β = 0.009 cm GW^{-1} [Fe ppm]$^{-1}$.

In each graph the solid line represents theoretical calculations made by solving Eq. 4. Values of a and b obtained by minimizing the error between calculation and experiment were calculated using the SOLVER routine in EXCEL. As can be seen a good fit is achieved with either the etched or non-etched data using the theory and these two parameters. However, both parameters are greater in the case of the non-etched data perhaps due to etching removing some surface contaminant but these differences could be experimental error from different samples. With all the data considered values of a and b are obtained of 0.013 cm^{-1} [Fe ppm]$^{-1}$ and 0.009 cm GW^{-1} [Fe ppm]$^{-1}$ respectively.

In order to insure that the absorption shown in Figs. 4-6 versus laser intensity is due to non-linear effects described by Eq. 1, and it is not due to the increase in fluence, the experiments were repeated using a longer pulse length, 7.8 nsec in place of 3.9. Single pulse shots were made at different points on the non-etched samples. The test fluence was increased by 1 J/cm^2 increments. The long pulse data is shown as diamonds in Fig. 8. When normalized to equivalent peak powers the data lies generally along the average of the scatter in data points from the 3.9 nsec pulse data. This comparison shows that transmission does depend on intensity or radiated power density. Also the many more data points obtained versus increasing intensity confirm the values of the non-linear parameters used in the theoretical fit to the combined data shown in Fig. 6.

A second important performance characteristic of an optical glass for laser applications is its resilience to successive laser shots. To determine whether successive shots would damage or solarize the glass samples, we measured the

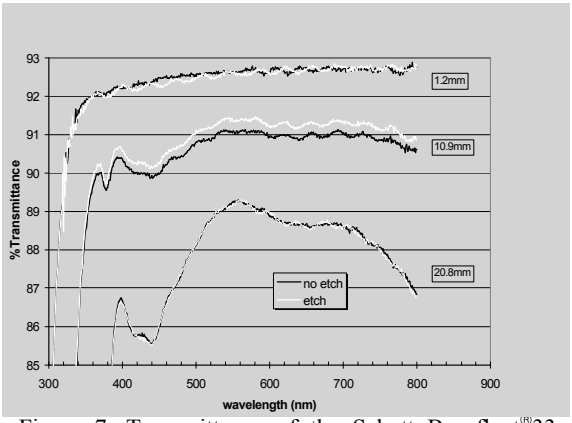

Figure 7. Transmittance of the Schott Borofloat®33 glass plates as a function of wavelength measured on the Cary spectrometer as described in the text. The spectra show no difference in the spectra between etched and non-etched samples.

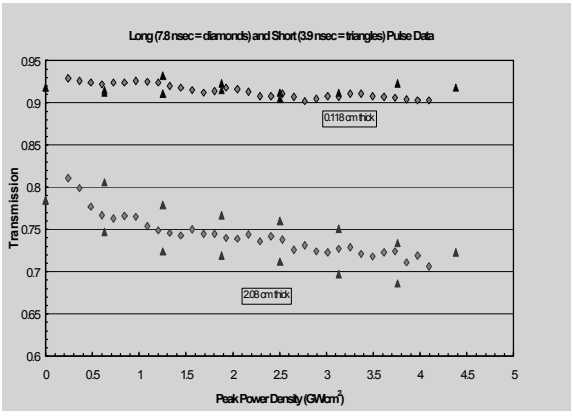

Figure 8. Comparison of transmission with a longer, 7.8 nsec, pulse width (diamonds) to data at equal peak intensities but shorter, 3.9 nsec pulse width (triangles).

cumulative degradation in transmittance. Twenty shots were made at one location on the plate measuring the transmission after each shot. The laser fluence was then incremented in steps of 1 J/cm^2 and the twenty shots repeated. This test was conducted on the plates of Schott Borofloat®33 glass with three different thickness: the A sample at 0.118 cm thick, the C sample, 2.08 cm thick, and an intermediate thickness sample at 0.33 cm thick. A 0.5 cm thick sample of BK7 glass was included in the set as a comparison. The results are shown in Fig. 9. These results show that although for the thicker samples transmission does decrease with increasing fluence as observed previously, there is little or no evidence of solarization over the twenty shots at each fluence except in the case of the BK7 sample. The latter shows significant evidence of cumulative damage over twenty shots at each fluence.

To further quantify the extent of solarization 100 shots were taken at one spot at each of several fluences with the longer pulse laser. Measurements were made at 2, 6, 10, 14, 18 and 22 J/cm^2. (22 J/cm^2 compares in intensity to 11 J/cm^2 for the shorter 3.9 nsec pulse.) The two non-etched samples, 0.118 and 2.08 cm in thickness, were used. For the thinner sample no evidence of solarization was present at any fluence level. For the thicker 2.08 cm sample solarization or a decrease in transmission with the number of shots is observed above 10 J/cm^2 or a peak intensity of 1.2 GW/cm^2. This can also be seen looking carefully at the 20 shot data of Fig. 9 above 5 J/cm^2. The dependence of solarization on sample thickness suggests that it is a bulk rather than surface effect.

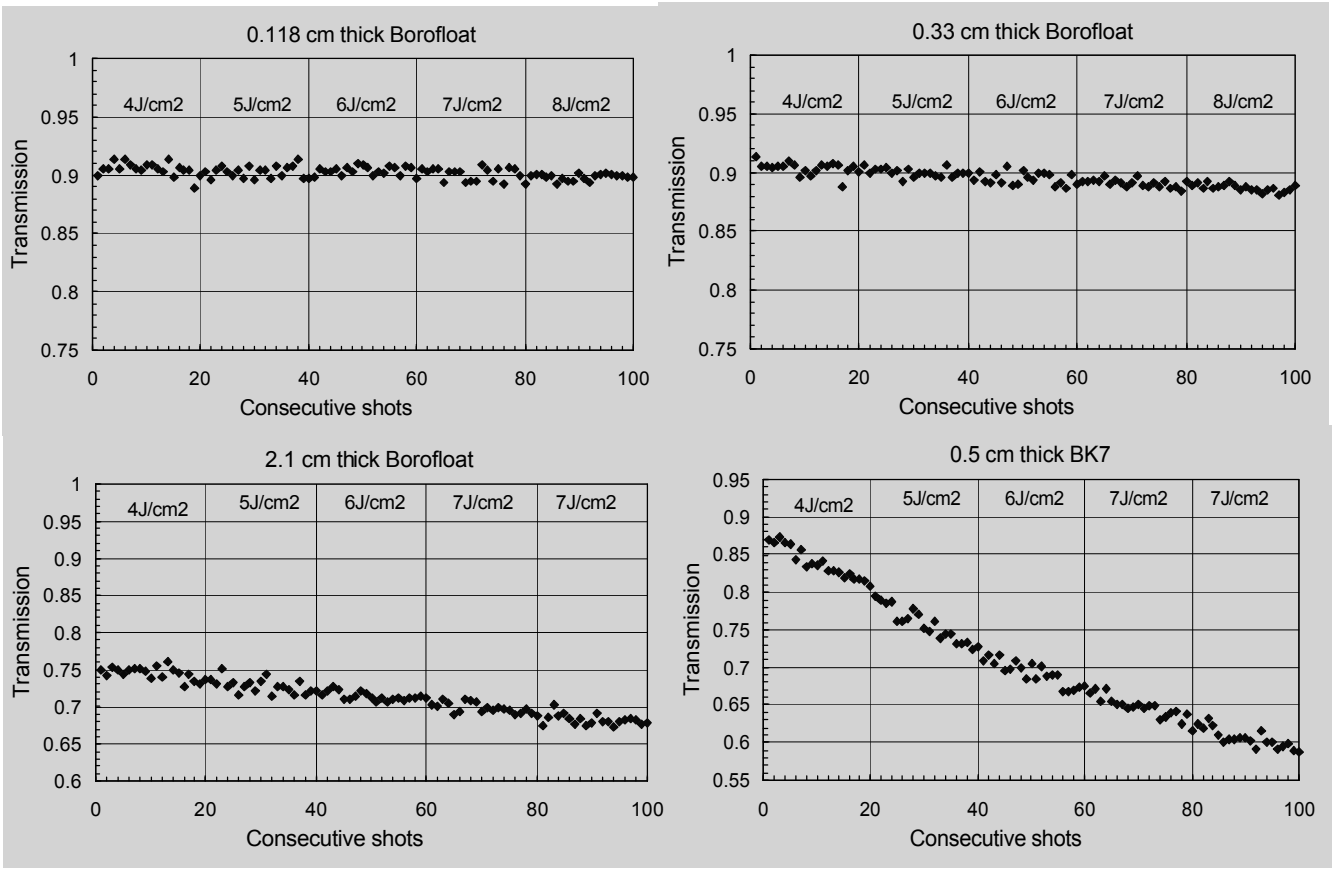

Figure 9. Results showing the cumulative degradation or loss in transmission versus the number of consecutive shots as the laser fluence is incremented every 20 shots. The 21 mm thick Borofloat®33 sample damaged at 8 J/cm^2, so the measurement was repeated with an additional 20 shots at 7 J/cm^2.

3.2 Impact of bulk flaws on laser performance

Due to both time and sample limitations, we have been able to test a limited number of bulk defects in 1mm thick Borofloat glass. Figures 10 and 11 show high resolution photomicrographs of bubbles, knots (high silica inclusions) before and after 351-nm laser irradiation to 10J/cm^2 and the corresponding fluence history for each defect. Laser irradiation produced no apparent change in the bubbles and knots. In order to observe the fluence at which damage initiated or grew on-line, and to confirm that damage truly initiated at the defect under study, we needed to be able to watch the defect while the sample was being laser-tested. Bubbles and inclusions caused significant phase aberrations which were readily detected in the beam nearfield image. Hence, it was not difficult to confirm the off-line microscope location of the defect and focus the on-line low-resolution microscope on the defect during laser irradiation.

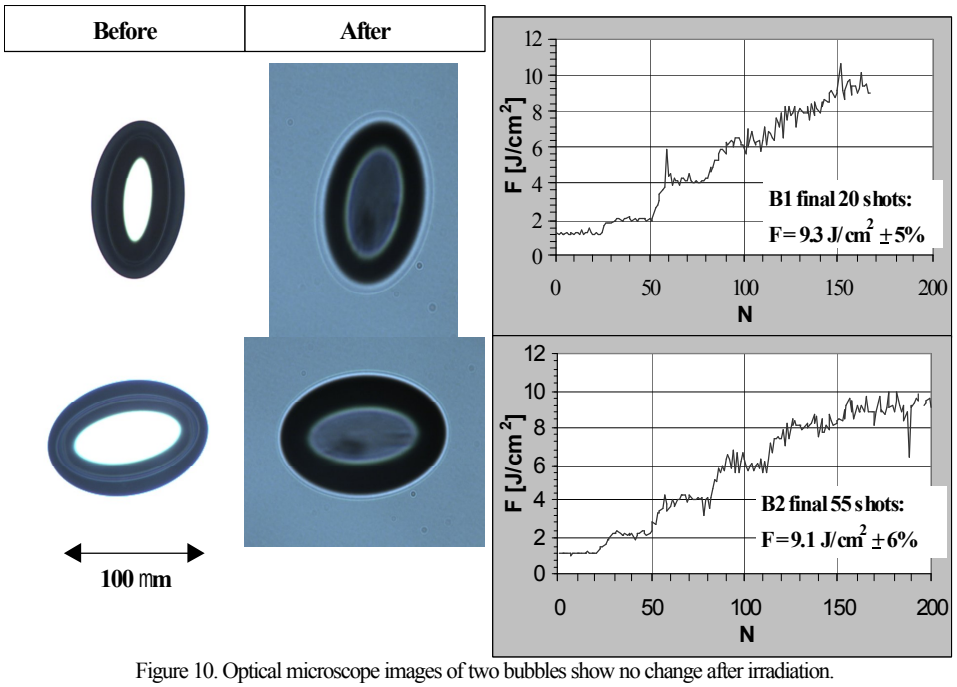

Figure 10. Optical microscope images of two bubbles show no change after irradiation.

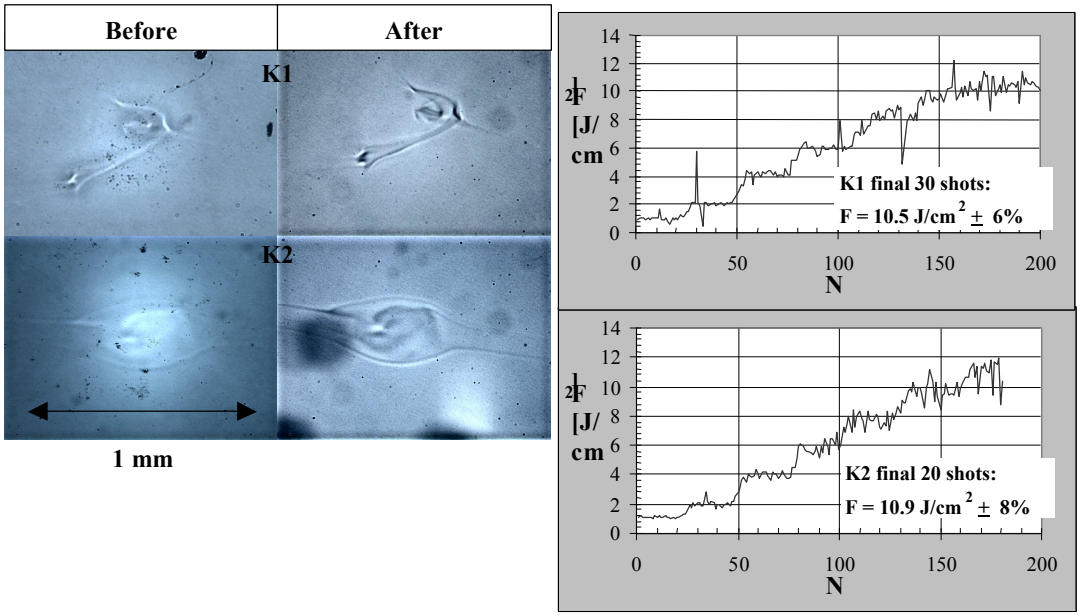

Figure 11. Optical microscope images of two knots show no changes after irradiance.

4. EFFECT ON FOCAL SPOT

The microfloat process used to manufacture the thin glass Borofloat®33 substrate produces very low microroughness. However, similar to drawn glass, the microfloat process produces a strongly 1-dimensional transmitted wavefront error perpendicular to the draw direction. Touch polish eliminates this wavefront error, producing a focal spot at the target which is indistinguishable from the original no-borosilicate optic case. Two full- aperture, 1mm thick touch-polished Borofloat®33 optics were shot on the NIF Precision Diagnostic System (PDS) beamline. The PDS beamline had a comprehensive suite of diagnostics, including a 3ω streak camera and near field and far field energy and power diagnostics, reactivated from the Beamlet Focal Plane Diagnostic [5]. The first optic was exposed to a 1 kJ, 1ns, flat-in-time (FIT) 351-nm pulse (0.9 J/cm2). The second optic transmitted a 2.5 kJ, 351-nm, 1ns FIT pulse (2.2 J/cm^2). As seen in Figure 16, the transmitted beam quality was not degraded by the thin borosilicate optic. There was no detectable energy loss on target, nor any detectable effect on the temporal or spatial pulse shape at either intensity. In addition, neither the on-line schlieren diagnostic images of the optic before and after the shot nor the off-line edge-lit high resolution full-aperture 'darkfield' photographs detected any change in the optic.

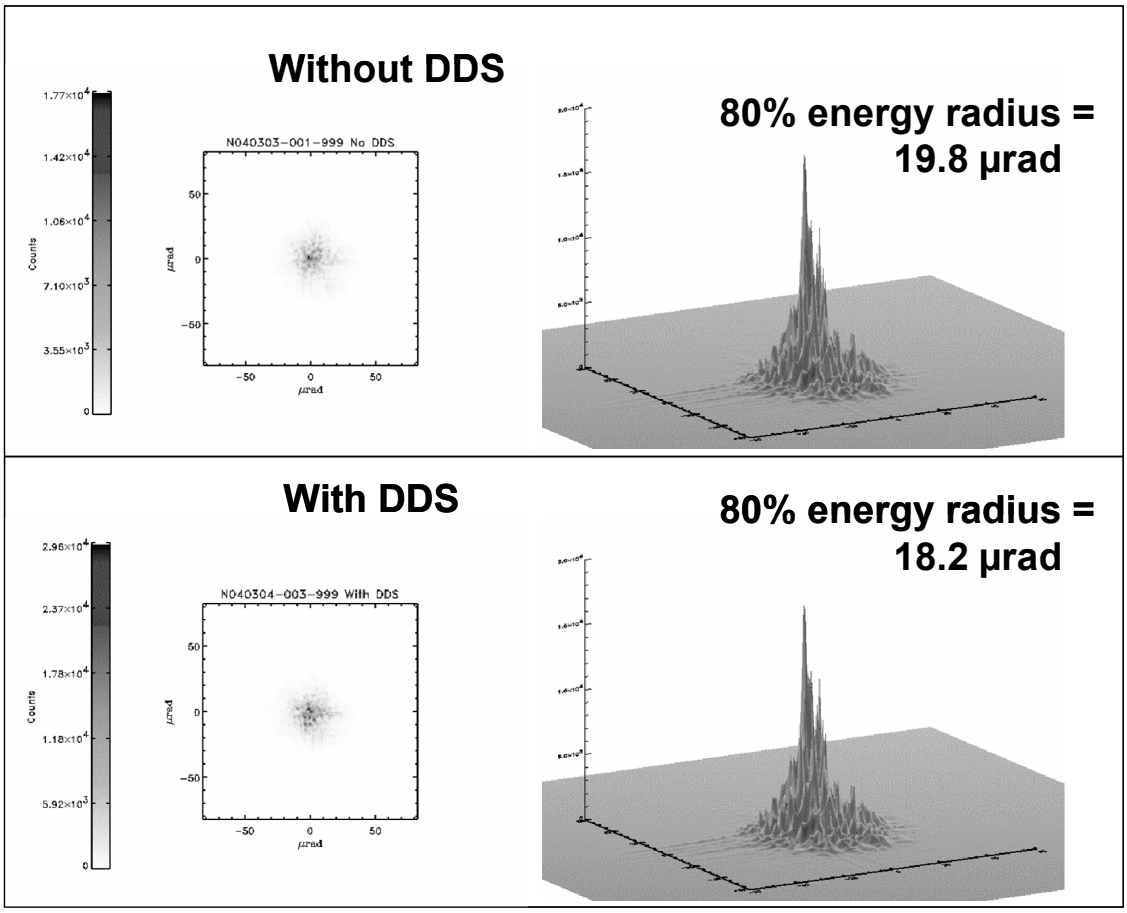

Figure 12. Comparison of the PDS 3ω focal spot at 1 kJ with and without a polished, 1mm Borofloat®33 "DDS" optic.

5. CONCLUSIONS

We have measured linear and non-linear absorption losses for Schott Borofloat®33 borosilicate glass. We find strong evidence for a reversible non-linear (intensity-dependent) absorption loss that is correlated with iron-impurity levels in the glass. We find negligible irreversible transmission losses due solarization for 1-mm thick Borofloat®33 samples for multiple 3ns, 355-nm pulses at fluences up to and including 8 J/cm^2. Preliminary data suggests that large bulk inclusions (bubbles and knots) exhibit little, if any, change upon 351-nm laser irradiation at fluences up to 10 J/cm^2. We conclude that touch-polished Borofloat®33 optics are a promising candidate to meet the beam energy and focus requirements for the NIF laser missions.

ACKNOWLEDGEMENTS

We wish to acknowledge the contributions of Jim Hughes, who conducted the XRF analyses, and Eric Miller who provided the spectrophotometer measurements, and Ron Luthi, who assisted in the design and procurement of the optics required to make these measurements on the SOT laser system.

This work was performed under the auspices of the U. S. Department of Energy by University of California, Lawrence Livermore National Laboratory under Contract No. W-7405-ENG-48

REFERENCES

[1] P. Whitman, M. Staggs, C.W. Carr, S. Dixit, W. Sell, D. Milam, "Performance of Thin Borosilicate Glass Sheets at 351-nm," *Laser-Induced Damage in Optical Materials: 2001*, SPIE Vol. 4679, 384-391 (2002).

[2] Whitman, P., Fair, J., Aboud, R., Burnham, A., Frieders, S., Thomas, I., Thorsness, C., "Improved Anti-Reflection Coatings for the National Ignition Facility Laser," ICF Quarterly Report, Vol. 9(2), UCRL-LR-105821-99-2, 163 - 176 (1999).

[4]C. B. Dane, L. E. Zapata, W. A. Neuman, M. A. Norton, and L. A. Hackel, 'Design and Operation of a 150 W Near Diffraction-limited Laser Amplifier with SBS Wavefront Correction," *IEEE J. Quantum Electronics*, 31, pp. 148-163, 1995.

[4] W. L. Smith, "Two-photon absorption in condensed media," CRC Handbook of Laser Science and Technology Vol. III: Optical Materials Part 1: Nonlinear Optical properties/radiation damage, M. Weber (ed.) CRC Press, Boca Raton, FL) pp. 229-258, 1986..

[5] P. J. Wegner, b. M Van Wonterghem, s. N. Dixit, M. A. Henesian, C. E. Barker, C. E. Thompson, L. G. Seppala, and J. A. Caird, "Characterization of third-harmonic target plane irradiance on the National Ignition Facility Beamlet demonstration project," *J. of Fusion Tech*., 30, 539-457 (1996).